

## Fuzzy PID Control-based Wheeled Tracing Robot

HUANG Dazhi\* and CHEN Jinsong

School of Mechanical Engineering, Huaihai Institute of Technology, Lianyungang 222005-CHINA  
Jiangsu Province R&D Institute of Marine Resources, Huaihai Institute of Technology, Lianyungang 222001-CHINA

Received 10 July 2013; Accepted 2 December 2013

### Abstract

Wheeled tracing robot is given increasingly high requirements in motion accuracy with its development. Therefore, it is of great significance in improving the control quality of wheeled tracing robot using appropriate controlling methods. Basing on analyzing the structure of wheeled tracing robot, this study established the kinematic and dynamic models of the robot. Moreover, by integrating the advantages of fuzzy algorithm and proportion-integration-differentiation (PID) algorithm, the robot is controllable by adjusting PID parameters using fuzzy algorithm. Test results verified the fuzzy PID control-based method was effective in controlling the wheeled tracing robot.

*Keywords:* Robot, Tracing, PID control, Fuzzy algorithm, Mathematical model.

### 1. Introduction

Wheeled tracing robot is capable of moving on purpose along preset paths and completing corresponding tasks being free of human intervention. As a typical mechatronics system built by mechanical system, power system, intelligent control system, and path recognition system, it plays an important role in fields of modern logistics and flexible manufacturing system [1],[2].

Control is a key field in the researches concerning wheeled tracing robot and also the basis for the positioning, navigation, and path-planning of robot. The controllers for high-velocity wheeled tracing robots are given higher requirements in real-time performance, stability, accuracy, and robustness [3],[4]. Therefore, it is necessary to establish the mathematical model to realize the control quality of wheeled tracing robot. Based on the analysis of mathematical model, this study employed a fuzzy PID method to control the motions of tracing robot and achieved desired controlling effect.

### 2. The Mathematical Models of Wheeled Tracing Robot

Wheeled tracing robots are mostly controlled by kinematic models, while the kinematic model-based control is established in conditions of low velocity, low acceleration, and low load. If the conditions above are unsatisfied, control accuracy will be weakened. Therefore, it is very necessary to build kinematic model of moving robot [5]. As a typical nonholonomic system, wheeled tracing robot faces more difficulties brought by nonholonomic constrains in dynamic modeling and trace tracking. Newton-Euler

method is modeling method being able of directly integrating nonholonomic constraints into equations [6]. Although the modeling using this method is more complex in case of more subcomponents, it is more applicable to the modeling of simple structures like the wheeled tracing robot investigated in this study.

### 2.1 Kinematic Model

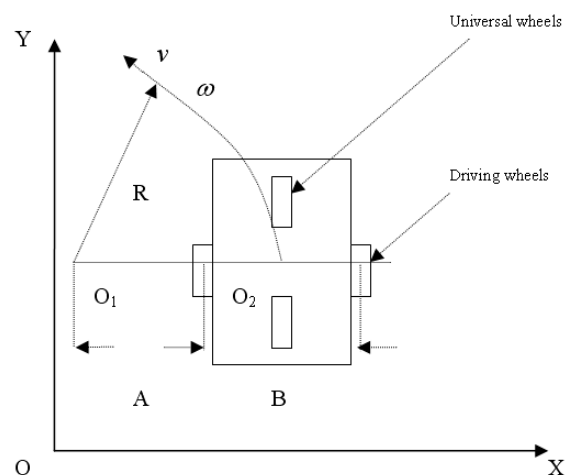


Fig. 1. The motion of robot.

Fig.1 shows the structure of the robot in this study. The robot is composed of a machine-structured mobile body structure, two driving wheels, and two following wheels. The two driving wheels are connected with two driving motors respectively. The motion of the robot is determined by the moving direction and

\* E-mail address: 2004000013@hhit.edu.cn

velocities of the two driving motors. The following wheels are universal wheels and used to support the robot motion and assist direction-adjustment. The movement of robot on ground can be decomposed into linear movement and rotation movement. In Cartesian coordinates, the position, velocity, angular velocity of robot can be represented by  $((x, y, \theta), v, \omega)$  respectively [7],[8]. The kinematic equation of robot is

$$\begin{bmatrix} \dot{x} \\ \dot{y} \\ \dot{\theta} \end{bmatrix} = \begin{bmatrix} \cos\theta & 0 \\ \sin\theta & 0 \\ 0 & 1 \end{bmatrix} \cdot \begin{bmatrix} v \\ \omega \end{bmatrix}$$

According to above equation, the attitude of the robot is controlled by the linear and angular velocities of the robot. However, linear and angular velocities are indirectly controlled by the moving direction and velocities of the driving motors. As shown in Fig.1, the robot is driven by the differential velocities of the two driving wheels. In this figure,  $v$  represents the moving velocity of the centroid (center)of robot;  $v_L$  refers to the movement velocity of the left driving wheel;  $v_R$  denotes the moving velocity of right wheel;  $A$  is the distance from the center of left wheel to the rotation center;  $B$  is the distance of the two driving wheels of the robot;  $\omega$  is the angular velocity of the centroid of robot. Therefore, the relationships of angular velocity and linear velocity with the velocities of the two driving motors are yield respectively:

$$v = \frac{v_R - v_L}{2}$$

$$\omega = \frac{v_R - v_L}{B}$$

Where,  $v_R = r\omega_R, v_L = r\omega_L$ , thus accelerations are  $\alpha_R = r\dot{\omega}_R, \alpha_L = r\dot{\omega}_L$ .  $r$  refers to the radius of the driving wheels, while  $\omega_R$  and  $\omega_L$  are the rotation velocities of the left and right driving wheels respectively.

By taking the derivations of above two equations, the acceleration and angular acceleration of the robot can be obtained:

$$\alpha = \frac{r(\dot{\omega}_R + \dot{\omega}_L)}{2}$$

$$\varepsilon = \frac{r(\dot{\omega}_R - \dot{\omega}_L)}{B}$$

## 2.2 Dynamic model

The dynamic mathematic model of the wheeled tracing robot was established on three parts: mobile body, driving wheels, and motors.

### Mobile body model

As shown in Fig.2, with the rotation center of the robot(on the connecting line of the centers of the two driving wheels)

as the coordinate origin, the stresses on the main body include the forces applied by the two driving wheels( $F_L, F_R$ ) and the gravity of the mobile body ( $m_b g$ ).

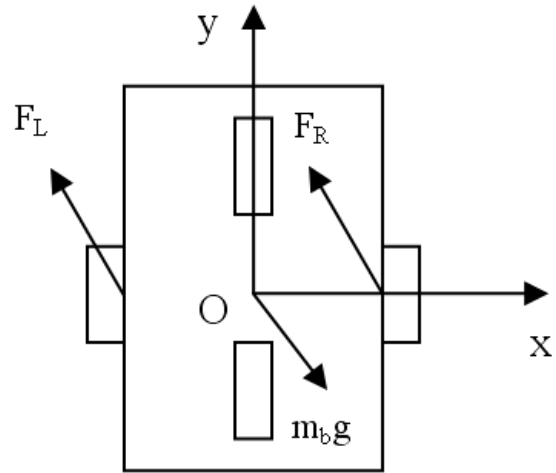


Fig. 2. The stresses on the mobile body.

The Newton - Euler equation of the mobile body is built:

$$\begin{cases} F_L^x + F_R^x = m_b \alpha \\ F_L^y + F_R^y = 0 \\ F_L^z + F_R^z = m_b g \\ \frac{F_R^x}{2} - \frac{F_L^x}{2} = J\varepsilon \end{cases}$$

Where,  $F_L^x$  and  $F_R^x$  represent the forces of  $F_L$  and  $F_R$  on axis of x respectively;  $F_L^y$  and  $F_R^y$  are the forces of  $F_L$  and  $F_R$  on axis of y respectively;  $F_L^z$  and  $F_R^z$  are the forces of  $F_L$  and  $F_R$  on axis of z respectively;  $J$  is the rotation inertia of robot wheels rotating around z axis.

### Driving wheels model

Fig.3 illustrates the coordinate established using the rotation center of the right wheel as origin. The forces on the wheels are consisted of torque  $M_{RW}$ , gravity  $m_w g$ , the force  $F_{RG}$  applied by ground on the right wheel, and the force  $F'_R$  loaded by mobile body to the right wheel. Among which, the latter two are a pair of active and reactive forces. Therefore,  $F'_R = F_R$ .

The Newton - Euler equation of the right wheel is established:

$$\begin{cases} F_R'^z = F_{RG}^z + m_w g \\ F_R'^x - F_{RG}^x = m_w a_R \\ F_R'^y = F_{RG}^y \\ M_{RW} - F_R'^x r = J_w \dot{\omega}_R \end{cases}$$

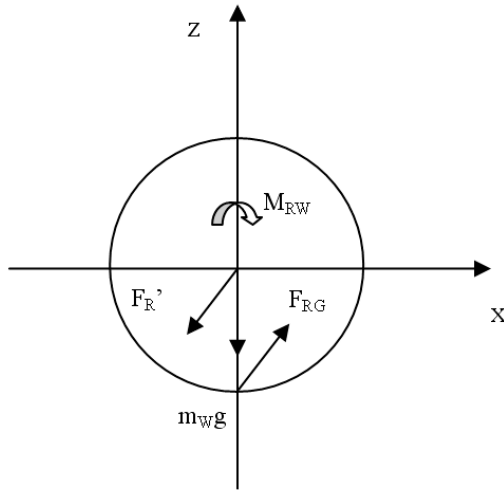


Fig. 3. The forces on the right wheel.

Where,  $J_w$  refers to the rotation inertia of the right driving wheel rotating around the center. Since the dynamics of the left and right driving wheels are identical, the dynamic equation of left wheel is shown as below:

$$\begin{cases} F_L'^z = F_{LG}^z + m_w g \\ F_L'^x - F_{LG}^x = m_w a_L \\ F_L'^y = F_{LG}^y \\ M_{LW} - F_L'^x r = J_w \dot{\omega}_L \end{cases}$$

**Dynamics of motor model**

Since the power of the robot is sourced from the driving force yield by motors, it is needed to analyze the motors. However, in the modeling process of wheeled robot, the dynamic characteristics of motors are usually neglected to simplify the design of controller. As a result, the controlling performance of the system is seriously affected. Therefore, to improve the controlling precision of the system, it is deemed to take account of the dynamic characteristics of motors. The motors used in the wheeled tracing robot in this study are DC servo motors. The dynamic characteristics from motor voltage to driving torque are expressed by the following equations.

$$M = k_M i$$

$$L \frac{di}{dt} + Ri + k_e \omega_M = U$$

Where,  $M$  is the driving torque of the motors;  $i$  is the armature current of the motors;  $k_M$  is the torque constant of the motors;  $L$  is the armature loop inductance of the motors;  $R$  is the armature circuit resistance of the motors;  $k_e$  is the back electromotive force constant of the motors;  $\omega_M$  angular velocity of the motors;  $U$  is the input voltage of the motors.

By integrating above two equations, the dynamic model of the motors with voltage as input variable is gettable

$$L \frac{1}{k_M} \frac{dM}{dt} + R \frac{M}{k_M} + k_e \omega_M = U$$

**The dynamic model of wheeled tracing robot**

According to the equations above, the dynamic equation of the wheeled tracing robot can be deduced

$$U = \begin{bmatrix} U_L \\ U_R \end{bmatrix} = \frac{L}{k_M} A \begin{bmatrix} \ddot{\omega}_L \\ \ddot{\omega}_R \end{bmatrix} + \frac{R}{k_M} A \begin{bmatrix} \dot{\omega}_L \\ \dot{\omega}_R \end{bmatrix} + k_e \begin{bmatrix} \omega_L \\ \omega_R \end{bmatrix}$$

Where,

$$A = \begin{bmatrix} J_w + m_w r^2 + \frac{r^2}{B^2} J + \frac{r^2}{2B} m_b & \frac{r^2}{2B} m_b - \frac{r^2}{B^2} J \\ \frac{r^2}{2B} m_b - \frac{r^2}{B^2} J & J_w + m_w r^2 + \frac{r^2}{B^2} J + \frac{r^2}{2B} m_b \end{bmatrix}$$

**2.3 Sensor model**

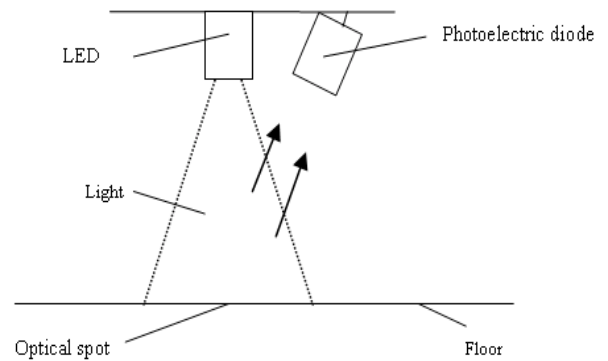


Fig. 4. The working principle of photoelectric sensor.

As shown in Fig.4, the luminous diode in diameter of 5 mm was opened with a hole in diameter of 3 mm on the top and preserved in dark. Through this hole, the lights emitted by the luminous diode concentrate into a circular spot in diameter of 10 mm on the ground being 20 mm away from the top of the luminous diode rather than scatter around. Moreover, the luminous diode, being rightly opposite to the spot, received the light signals reflected form the ground. The sensor can work normally in ground gray scale above 40% (0% is white, 100% is black) and navigation line gray scale below 10%. When the spot reached to the ground, the lights reflected were processed into high level signals since they were too weak to conduct the photoelectric diode under the high ground gray scale. When the spot arrived at the navigation line, the light reflected were processed into low level signals since they were intensive enough to conduct the photoelectric diode under the low gray scale of navigation line. Test result suggests that, in stable light environment, the sensor was most stable and reliable when half of the spot lying on the navigation line and the lights reflected were processed into low level signals.

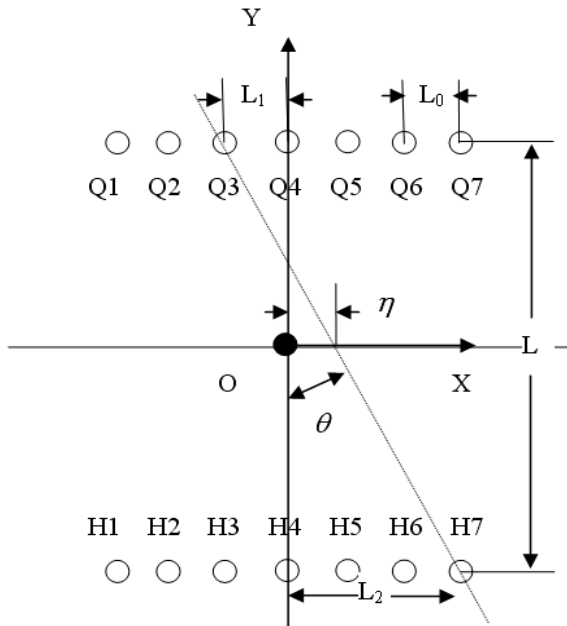


Fig. 5. The layout of photoelectric diode.

Fig.5 shows the layout of the photoelectric diode. The motion coordinate system of the robot was established using the horizontal center line of the robot as x axis, the longitudinal center line as y axis, and the robot center as origin. In Fig.5, the circle represents the spot formed by the light emitted from diode on the ground. Obviously, there are 7 photoelectric sensors (in two rows) symmetrically placed on the front and back of the robot in vertical distance of L. The thin solid line with a certain angle with y axis is the center line of the navigation line that should be followed by robot. By detecting the derivation (L1and L2) of the robot axes from the navigation line using photoelectric sensors on the front and back, the angle  $\theta$  and center offset  $\eta$  of the robot can be obtained. The relationships of  $\theta$  and  $\eta$  with L1 and L2 are indicated as follows:

$$\eta = \frac{L_1 - L_2}{2}$$

$$\theta = \arctan\left(\frac{L_1 + L_2}{L}\right)$$

The above two equations imply that  $\eta$  is unrelated to L, while  $\theta$  is inversely proportional to L. Therefore, the increase in the length of the robot is beneficial to the attitude adjustment of robot.

The sensors were arranged in isometric space of (20 mm). To facilitate the processing of computer, the sensors were numbered as -3, -2, -1, 0, 1, 2, and 3 from left to right in sequence. Then using above tow equations, the deflection and the center offset can be acquired and used to correct the attitude of robot.

**3. Fuzzy PID Control**

Although we have established the mathematical model of wheeled tracing robot, the model is incapable of completely

accurately describing the practical situation since it is established basing on many hypotheses. Therefore, the PID control, which greatly relies on accurate mathematical model, cannot yield desired effect using the model above. In case of using the fuzzy control with low requirement in mathematical model, some problems, such as low accuracy and the unsmooth situation in control process are prone to be induced [9]. Therefore, in this study, the advantages of the PID algorithm and fuzzy algorithm are combined by dynamically adjusting the parameters of PID algorithm using fuzzy algorithm. In this way, more desired control effect can be yield.

Fig.6 is a block diagram of the fuzzy PID control system of robot. The two rows of sensors on the front and back are used to detect the attitude of robot. According to the sensors models, the attitude offset can be figured out. Then using the inverse kinematic model of robot, the derivations in rotating speeds of the right driving wheel and left driving wheel are gettable. Subsequently, according to the rotating speed derivation of right and left wheels and related variation rates, the PID control parameters can be acquired in the adjusting module of fuzzy parameter. In such way, the right and left motors are accurately controlled by PID controller and the attitudes of tracing robot are adjustable in turn. Finally, tracing robot can move along the preset tracks.

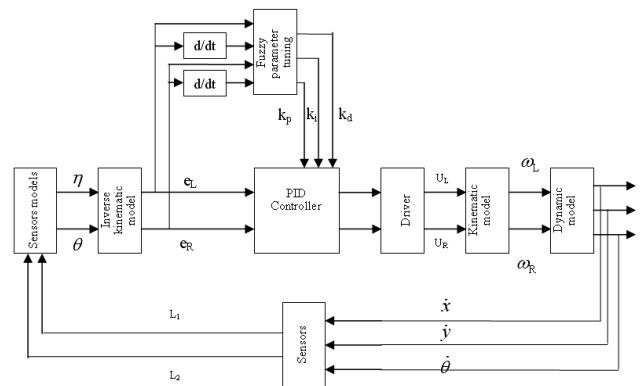


Fig. 6. The fuzzy PID control system.

**3.1 Defining fuzzy variables**

Analysis on the principle of fuzzy PID control system of the wheeled tracing robot suggested that the fuzzy PID parameters adjusted included the rotating speed derivation of the right and left wheels (eL and eR) and related variation rates (ecL and ecR), while the parameters output contained the kp, ki, kd needed by PID controller. Since the control methods of right and left driving wheels were identical, this study exemplified left driving wheel to explain how fuzzy PID control was realized.

**3.2 Fuzzification**

The signals collected by sensors were firstly calculated by sensor models. The results obtained were further computed by inverse kinematic model to yield the deviation of left driving wheel eL. and corresponding variation rate ecL. The eL and ecL obtained were used as the basic input variables of fuzzification. Under fuzzy domain of [-1,1], fuzzy variables were corresponded into 5 grades [-1, -0.5, 0, 0.5, 1]. Subsequently, according to membership functions, the five grades were expressed into 5 fuzzy subsets valued by the fuzzy variables in symbols of NB, NM, O, PM, and PB. In accordance with the membership functions in Fig.7, NB was a Z-typed membership function, PB was a S-typed

membership function, while the other three were triangular membership functions.

Tab.1. The adjusting rules for PID parameters

PID	ec					
	NB	NM	O	PM	PB	
e	NB	PB Z PS	PL Z PS	PL Z PS	PB Z PS	PB Z PS
	NM	PS PB PB	PM PM PB	PB PS PL	PM PM PB	PS PB PB
	O	PB PB PS	PB PB PM	PL PM PB	PB PB PM	PB PB PS
	PM	PS PB PB	PM PM PB	PB PS PL	PM PM PB	PS PB PB
	PB	PB Z PS	PL Z PS	PL Z PS	PL Z PS	PB Z PS

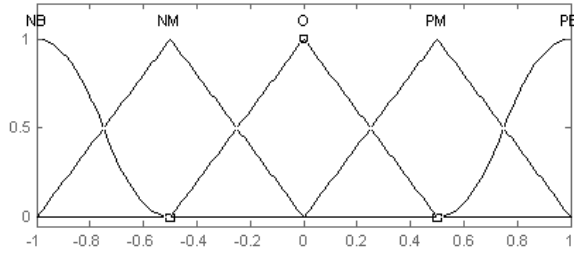


Fig. 7. The membership function of input variables.

The  $k_p$ ,  $k_i$  and  $k_d$  needed by PID controller were used as the basic output variables of fuzzification. Under fuzzy domain of [0, 1], fuzzy variables were corresponded into 5 grades [-1, -0.5, 0, 0.5, 1]. Subsequently, according to membership functions, the five grades were expressed into 5 fuzzy subsets valued by the fuzzy variables in symbols of Z, PS, PM, PB, and PL. In accordance with the membership functions in Fig.8, Z was a Z-typed membership function; PL was a S-typed membership function, while the other three were triangular membership functions.

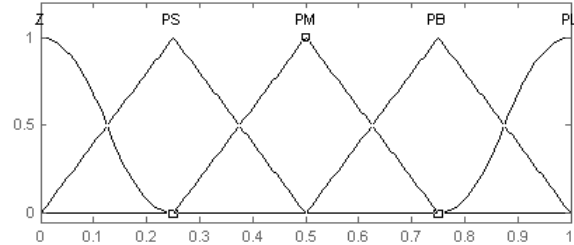


Fig. 8. The membership functions of the output variables.

3.3 Fuzzy rules

According to the classical theory of PID control, fuzzy rules are established as follows:

- (1) In case of larger  $|e|$ , we take larger  $k_p$ , zero in  $k_i$ , and smaller  $k_d$ .
- (2) In case of medium  $|e|$  and  $|ec|$ , we take smaller  $k_p$  and moderate  $k_i$  and  $k_d$ .
- (3) In case of smaller  $|e|$ ,  $k_p$  and  $k_i$  should be increased, while  $k_d$  should be reduced with the increase of  $|ec|$ .

Corresponding control rules can be interpreted using the fuzzy conditional statements below.

IF  $e=NB$  AND  $ec=NB$  THEN  $k_p=PB$ ,  $k_i=Z$ ,  $k_d=PS$   
 IF  $e=NB$  AND  $ec=NM$  THEN  $k_p=PL$ ,  $k_i=Z$ ,  $k_d=PS$   
 ...

IF  $e=O$  AND  $ec=NB$  THEN  $k_p=PB$ ,  $k_i=PB$ ,  $k_d=PS$   
 IF  $e=O$  AND  $ec=NM$  THEN  $k_p=PB$ ,  $k_i=PB$ ,  $k_d=PM$   
 ...

Similarly, all the 25 control rules can be simplified into a fuzzy control rule table (Tab.1).

3.4 Defuzzification

According to the values of  $e$  and  $ec$  and related fuzzy rules, the  $k_p$ ,  $k_i$ , and  $k_d$  needed by PID controller were gettable. Then by experience, they were multiplied with corresponding coefficients (20, 0.1, and 0.5) separately and then input into PID controller to adjust the control parameters to achieve the optimal control effect.

4. Test

As shown in Fig.9, the wheeled tracing robot with weight of 2 Kg is powered by two 10 W DC servo motors with maximum rotating speed of 2700 r/m. The driving wheels in diameter 40 mm were driven by the output shaft of each motor via the 9:1 reducer.

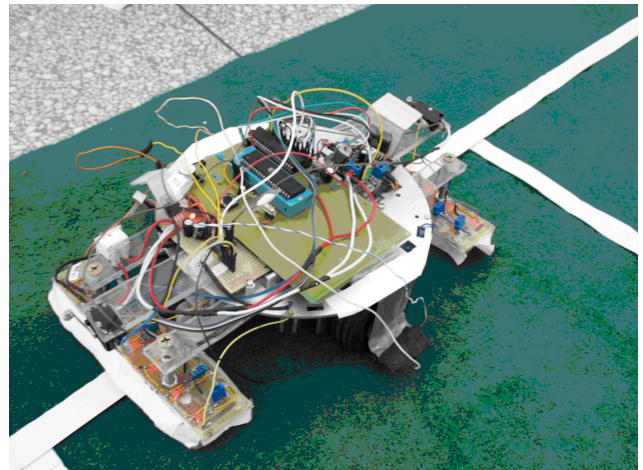
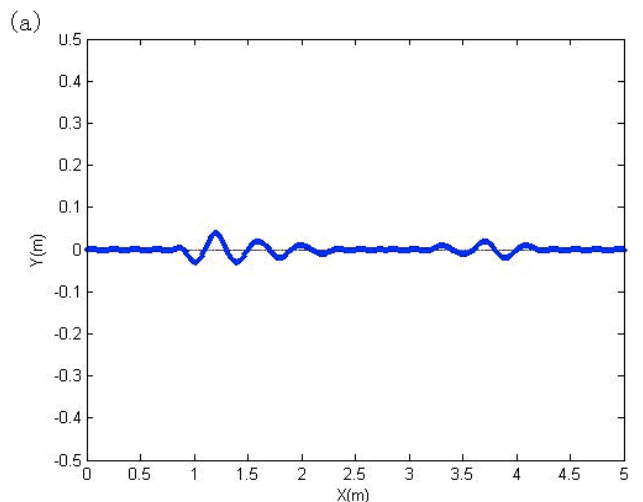


Fig. 9. The tracing of robot.

Under the 5 m linear tracing of robot at the average moving speed of 0.5 m/s, 0.3 m/s, and 0.1 m/s, the moving tracks of the center of robot are shown in Figure 10 (a), (b), (c) respectively.



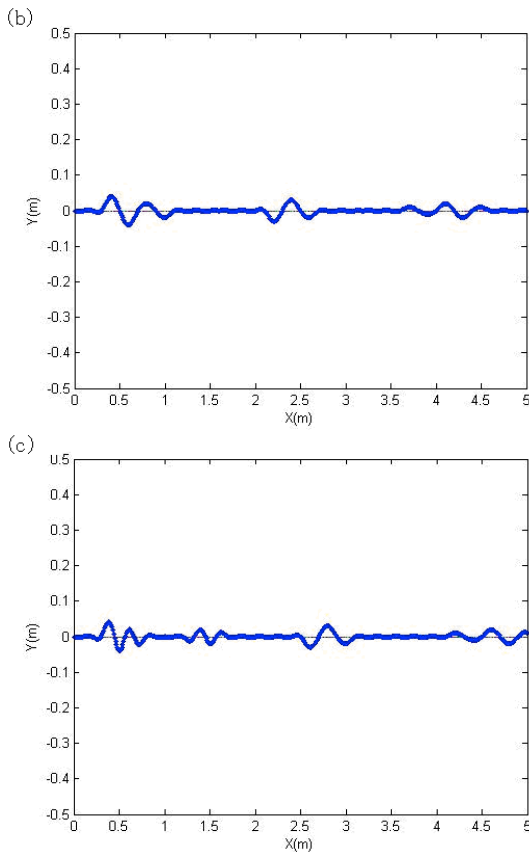


Fig. 10. Diagram of the tracing robot center.

As shown in Fig.10, with the decrease of average speed, wheeled tracing robot showed more adjustment times. But the adjustment duration was shortened to some extent. In whole, the robot presented swings (with error in 0.005 m) in its linear movements regardless of the average speed. However, the robot could recover to the stable state in short time period and then moved ahead in full speed. Test result proved that fuzzy PID control algorithm achieved good results when used to control the motions of tracing robot.

## 5. Conclusions

- 1) By analyzing the structure of the wheeled tracing robot, the kinematic and dynamic models of the robot were built.
- 2) To achieve more accurate control effect to the robot, the PID parameters were dynamically adjusted using fuzzy algorithm.
- 3) The test results proved the PID control-based wheeled tracing robot achieved satisfactory control effect.

## 6. Acknowledgment

The authors thank that the study is supported by A Project Funded by the Priority Academic Program Development of Jiangsu Higher Education Institutions and the National Science Foundation of China (No. 51105204 and 51105162).

## References

1. Demirli K, Khoshnejad M, "Autonomous parallel parking of a car-like mobile robot by a neuro-fuzzy sensor based controller", *Fuzzy Sets and Systems* 160(19), 2009, pp.2876 -2891.
2. Ch.K.Volos, I.M.Kyprianidis, I.N.Stouboulos, "Motion Control of Robots Using a Chaotic Truly Random Bits Generator", *Journal of Engineering Science and Technology Review* 5(2), 2012, pp. 6-11.
3. GAO Junyao, LU Jilian, "Steering Control of Wheeled Mobile Robot Using GA Fuzzy Neural Network", *Transactions of Beijing Institute of Technology* 23(2), 2003, pp.176-180.
4. GONG Jianwei, GAO Junyao, LU Jilian, "Heading-following control of a wheeled mobile robot in sharply curved roads", *Journal of Beijing Institute of Technology* 21(6), 2001, pp.680-683.
5. CHEN Xiaopeng, LI Chengrong, LI Gongyan, etc, "Dynamic Model Based Motor Control for Wheeled Mobile Robots", *Robot* 30(4), 2008, pp. 326-332
6. XIA Tian, LI Yizhong, JIN Chao, etc, "College of Mechanical and Electrical Differential Steering Dynamic Analysis and Simulation of AGV", *Coal Mine Machinery* 33(3), 2012, pp. 63-64.
7. HUANG Dazhi, ZHOU Qinggui, CHEN Yeqi, "The Design of Control System for Tracing Robot", *MACHINE TOOL&HYDRAULICS* 37(8), 2009, pp.350-352.
8. HUANG Dazhi, ZHANG Yuanliang, "Fuzzy Control of Intelligent Tracing Vehicles", *Information Technology Journal* 12(10), 2013, pp. 2016-2022.
9. HESSBURG T, TOM IZUKA M, "Fuzzy logic control for lateral vehicle guidance", *IEEE Control System Magazine*, (4), 1994, pp.300- 313.
10. B. S. Reddy, "Prediction of Surface Roughness in End Milling of P20 Mould Steel Using Artificial Neural Networks", *Journal of Engineering Science And Technology Review*, 5(1),2012,pp. 1-6.